SEMARAK ILMU PUBLISHING

Journal of Advanced Research in Applied Sciences and Engineering Technology

Journal homepage:
https://semarakilmu.com.my/journals/index.php/applied_sciences_eng_tech/index
ISSN: 2462-1943

Hybrid One-Cycle-PI Control Algorithm for Shunt Active Power Filter in Mitigating Harmonic Currents

Nurul Izzah Mohamad Ariffin[1], Nor Farahaida Abdul Rahman[1,*], Siti Zaliha Mohammad Noor[2]

[1] School of Electrical Engineering, College of Engineering, Universiti Teknologi MARA, 40450 Shah Alam, Selangor, Malaysia
[2] Solar Research Institute, Universiti Teknologi MARA, 40450 Shah Alam, Selangor, Malaysia

ARTICLE INFO

Article history:
Received 15 May 2023
Received in revised form 13 September 2023
Accepted 25 September 2023
Available online 15 October 2023

Keywords:
Shunt Active Power Filter (SAPF); One-Cycle Control (OCC); Hybrid One-Cycle-PI Control (HOCPIC); Total Harmonic Distortion (THD)

ABSTRACT

The quality of current waveforms, such as the presence of the harmonic components at the point of common coupling of various consumers, deteriorated due to the nonlinear load applications. Hence, a Shunt Active Power Filter (SAPF) is used to mitigate harmonic pollution in an electrical network. The heart of the SAPF operation is the current control technique. The choice of current control techniques significantly impacts the SAPF performance. As a result, a Hybrid One-Cycle-PI Control (HOCPIC) is proposed to work as a single-phase SAPF's current controller. The HOCPIC utilises a Proportional-Integral (PI) controller to minimise the error signal. As a result, the THD value of the supply current is reduced to 3.20% using the SAPF-based HOCPIC compared to 3.99% when using the SAPF-based OCC. The result proves that the SAPF-based HOCPIC performs better in compensating harmonic currents than the SAPF-based OCC.

1. Introduction

Nonlinear electric appliances, which rely on power electronic switches, are widely used worldwide [1]. The utilisation of nonlinear loads, such as personal computers, line-switched rectifiers, and arc furnaces, gives rise to power quality problems such as current harmonics [2,3]. It happens when the AC voltage or current waveform consists of integral multiple AC components of the fundamental device frequency [4]. Subsequently, it can cause excessive neutral currents, equipment overheating, motor vibration and capacitor blowing [5]. Thus, one of the techniques to compensate for the harmonic components is Shunt Active Power Filters (SAPFs) [6]. A SAPF is an efficient mitigation tool compared with a passive filter due to its capability to simultaneously compensate for multiple harmonic currents [7,8]. It is connected in parallel with the nonlinear loads to act as a voltage or current source to compensate for the harmonic components in the line current; it results in a sinusoidal line current that is in phase with the grid voltage [9]. SAPFs consist of fast inner current control algorithms to regulate the current injected into the power grid while maintaining the prescribed Total Harmonic Distortion (THD) and Power Factor (PF) [10,11]. The power quality injected

* *Corresponding author.*
E-mail address: farahaida@uitm.edu.my

https://doi.org/10.37934/araset.33.1.3143

into the grid and the converter system's performance depends on the inverter's current control algorithm [12].

As a result, the One-Cycle Control (OCC) scheme is dedicated to this project which focuses on the current control algorithms to generate switching pulses for the SAPF. Initially, OCC was proposed by K. M. Smedley *et al.,* in [13] to regulate switching converters with one switching cycle. After a transient, the controller achieves immediate dynamic control of the average value of the switching variables. The OCC technique achieves instantaneous control over the average value of the chopped voltage or current by utilising the pulsed and nonlinear nature of switching converters. The OCC method offers rapid dynamic response and excellent input-perturbation rejection. It is appropriate for controlling Pulse Width Modulated (PWM) and Quasi-Resonant (QR) converters. The OCC strategy showed great promise featuring excellent harmonic suppression, simple circuitry, robust performance, fast response, extensive stability range, reliability, universal, and low cost for the control of SAPF [13,14].

In SAPF operations, the conventional OCC concept has been widely employed. Huaiying *et al*., [15] created a simulation model of a single-phase SAPF with OCC operating under bipolar modulation. OCC was selected as the control approach to mitigate AC power grid pollution caused by harmonic and reactive power. Furthermore, some researchers in [16, 17] prefer to use a modified OCC rather than a conventional OCC to obtain dynamic SAPF performance with fewer sensors. A fast response OCC (FOCC) strategy for APF was proposed to improve existing OCC strategies. The analysis, design procedure, and auxiliary schemes for a triangular carrier generator and an integrated current/voltage sensor were presented. Verification was performed throughout the simulation, and the results show that the proposal's performance was significantly better than the conventional technique. The researchers claimed that FOCC is required fewer devices and lower costs. Nonetheless, the design is complicated and does not adhere to the original OCC concept.

The researchers described the waveforms of the SAPF-based OCC for the carrier waveform, modulating waveform, and gating signal in [18-22]. However, no explanation is provided for the effect of clock pulse width because it is only used to initiate the control pulses. Nonetheless, the researcher can achieve the desired result even with a short clock pulse width. Hence, it indicates that no research has been done on the effect of clock pulse width on conventional OCC in SAPF. Thus, it is worth studying OCC's clock pulse width on SAPF operation to observe the effect of clock pulse width on the THD of supply current. The THD of a waveform reveals how many unwanted components are present in the signal. As the THD of a waveform increases, the signal contains a more significant number of undesired components [23].

In the conventional OCC, the comparator results of the integrated injection current and error current signal determine the conventional OCC controller output. However, the controller performs poorly because conventional OCC cannot tune the error signal dynamically. Therefore, Li *et al.,* [24] used a hybrid modified OCC-PI, where the Proportional-Integral (PI) controller will minimise the error signal and eventually improve the controller operation. However, unlike the conventional OCC, the hybrid-modified OCC does not generate control pulses directly from the S-R flip flop. Instead, additional components are required to generate the control pulses. Hence, it increases the complexity of the controller.

Saifullah Khalid has published several scholarly articles on the control technique of PI controllers, including the Adaptive Mosquito Blood Search Algorithm (AMBS), Adaptive Tabu Search Algorithm (ATS), and Adaptive Spider Net Search Algorithm (ASNS). In [25], he introduced the AMBS to enhance the conventional control scheme utilised in SAPF and explore the optimal values of PI controller parameters, which has resulted in a remarkable reduction in the THD of the supply current and voltage. Additionally, his implementation of the ATS to search the PI controller parameters to

mitigate the adverse effects of nonlinear loads on the aircraft's electrical system, which utilise an Artificial Neural Network (ANN) in [26], and a fuzzy logic controller in [27] at 400 Hz is noteworthy. Moreover, Saifullah Khalid also introduced the ASNS in [28] to search for the optimum value of the proportional integral controller parameters and the objective function is determined in such a way that their optimum value is given with the conditions of % overshoot, rise time, and settling time. The algorithm offers notable advantages due to its ease of use, programmability, feasibility, and reduced computational time. Subsequently, the ASNS was implemented in SAPF for aircraft supply systems [29].

Based on the limitations of previous work, this paper provides new insights into studying the impact of OCC's clock pulse width on the operation of SAPF. The paper also focuses on developing a SAPF-based Hybrid One-Cycle-PI Control (HOCPIC), which combines the conventional OCC with the PI controller to improve the SAPF mitigation by minimising error signals and providing more dynamic performance. The proposed hybrid controller can compensate for the harmonic components of the supply current and will have a simpler architecture because it retains the basic OCC structure. Furthermore, analytical investigations, followed by thorough simulation studies, are conducted to determine the efficacy of the proposed plan.

2. Single-Phase Shunt Active Power Filter

Figure 1 depicts the operation of the SAPF connected at a Point of Common Coupling (PCC) of the grid source, which supplies power to the nonlinear load. The nonlinear load operation draws the instantaneous nonlinear load current $i_L(t)$, which comprises the instantaneous fundamental current $i_F(t)$ and the instantaneous harmonic current $i_H(t)$ components. The SAPF supplies instantaneous injection current $i_{inj}(t)$ to compensate for the harmonic components of $i_L(t)$; the $i_{inj}(t)$ has the same amplitude as the harmonic components as $i_L(t)$ but opposite polarity. The SAPF also draws instantaneous current $i_{dc}(t)$ to charge the DC-link capacitor. This statement can be expressed as in Eq. (1) until Eq. (4).

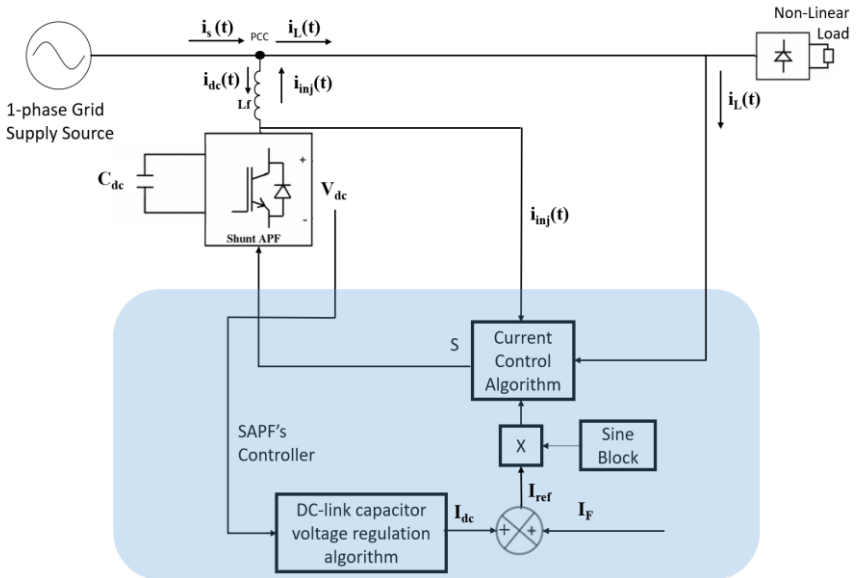

Fig. 1. The schematic diagram of single-phase nonlinear load integrated with SAPF

$$i_L(t) = i_F(t) + i_H(t) \tag{1}$$

$$i_{inj}(t) = i_H(t) \tag{2}$$

According to Figure 1,

$$i_s(t) = i_L(t) - i_{inj}(t) + i_{dc}(t) \tag{3}$$

Substitute Eq. (1) and Eq. (2) into Eq. (3)

$$i_s(t) = i_F(t) + i_H(t) - i_H(t) + i_{dc}(t)$$
$$i_s(t) = i_F(t) + i_{dc}(t) \tag{4}$$

According to Eq. (4), the supply current $i_s(t)$ waveform no longer has harmonic components when the power system applies the SAPF. The SAPF applies a current control algorithm to regulate $i_{inj}(t)$. Additionally, the filter employs a voltage control algorithm to maintain a constant voltage V_{dc} across the DC-link capacitor (C_{dc}). The C_{dc} is discharging when V_{dc} is positive, which indicates that the SAPF supplies $i_{inj}(t)$. Meanwhile, the C_{dc} is charging when V_{dc} is negative, which means that the SAPF draws $i_{dc}(t)$ from the grid. When the desired voltage is on point, hence, $i_{dc}(t)$ equals zero. A PI controller is used in the voltage regulation algorithm to eliminate the steady-state error of V_{dc} by tracking the voltage based on the reference voltage value V_{dc_ref} [1].

3. Development of The Current Control Algorithm

3.1 Current Control Algorithm based on OCC

Figure 2 shows the SAPF's current control algorithm using a conventional OCC; the main component is the integrator and the resetter. At the beginning of each switching period, a constant frequency clock turns on the Insulated-gate Bipolar Transistor (IGBT). At this moment, the integration also starts to operate. The injection current is integrated and compared with the error current signal of the injection current and reference injection current. The comparator changes its state as soon as the integrated injection current reaches the error current signal. The controller sends a command to the switch to change the transistor from the on-state to the off-state. At the same time, the controller reset the integrator to zero.

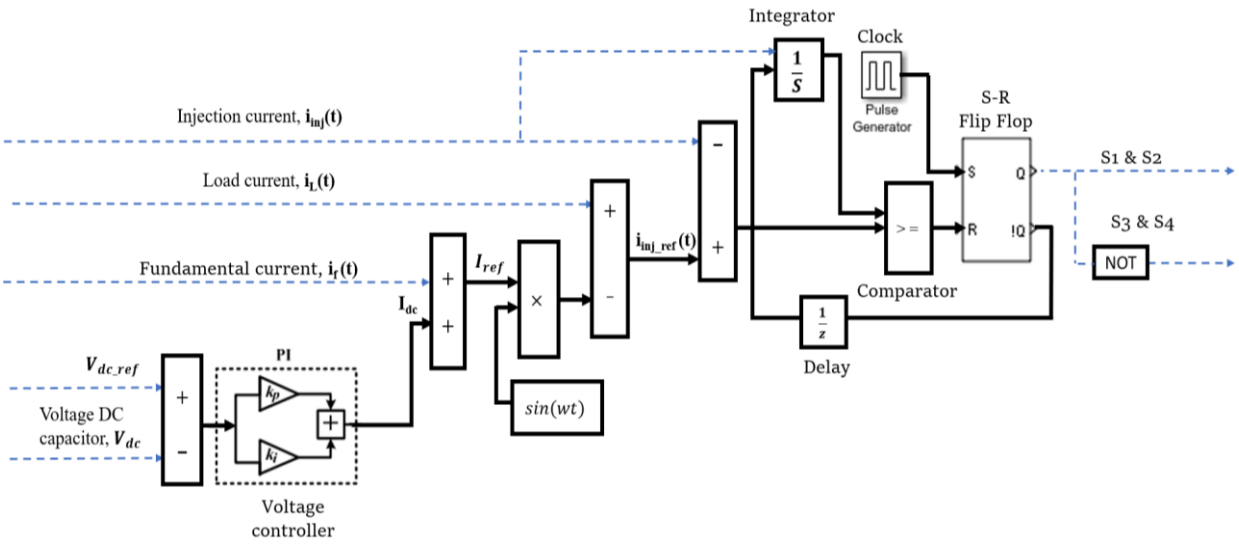

Fig. 2. The schematic diagram of SAPF's current control algorithm using conventional OCC

3.2 Current Control Algorithm based on HOCPIC

Figure 3 presents the schematic diagram of SAPF's current control algorithm using HOCPIC. The conventional OCC is a hybrid with a PI controller. The PI controller is used to minimise the error of the injection current. This simulation uses trial-and-error tuning to determine the optimal gains for the Kp and Ki that provide robust performance, rapid dynamic response, and reduced steady-state error. The gains were determined based on the lowest THD value of $i_s(t)$ compensated by the SAPF. Although no specific tuning algorithm was used, the PI controller could still regulate the SAPF operation. This is due to the systematic tuning procedures supported by papers in [30, 31] that used the same tuning method to tune the conventional PI controller to achieve the desired response.

The pulse of HOCPIC will start at the beginning of each switching time. Once the clock starts, the integration begins. In this simulation, the integrator will integrate when it receives a raising, which is '1'. The clock triggers the S-R flip flop to generate control pulses to the SAPF's power switches (S1&S1, S3&S4). The injection current is integrated and compared with an improved error current signal. Before it is compared, the error current signal has been minimised with the help of the PI controller. When the integrated value of the injection current reaches the improved error current signal, the comparator changes its state, resets the S-R flip-flop, and, consequently, generates the control pulses.

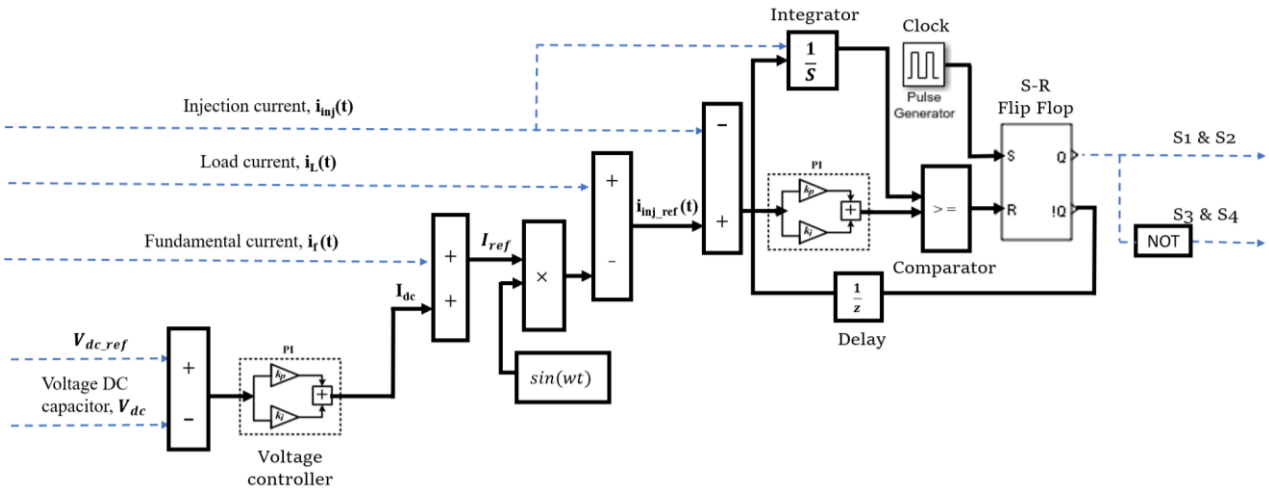

Fig. 3. The schematic diagram of SAPF's current control algorithm using conventional HOCPIC

4. Results and Discussions

The proposed model is simulated using MATLAB /Simulink Software. Table 1 shows the simulation parameters of the SAPF system connecting to the PCC of single-phase nonlinear load.

Table 1
The Parameters and Components for SAPF

Simulation Parameters	Value
RMS Supply Voltage (Vs)	230 V
Frequency of Input Voltage	50 Hz
Switching Frequency	25 kHz
Line Inductor	2 mH
Injection Inductor	10 mH
DC Link Capacitor	3700 mF
DC-Link Reference Voltage	450 V
PI Voltage Controller	Kp=0.35, Ki=0.35
Nonlinear Load (Resistor/Inductance)	70 Ω / 0.8 H
Pulse Generator	Period=6 samples
PI Controller in HOCPIC	Kp=1.9, Ki=1.26

4.1 Effect of Using Various OCC's Clock Pulse Width on The SAPF Performance

The output of the comparator triggers the S-R flip-flop during each clock cycle, thereby stabilising the system. Based on this analysis, the duty ratio sequence converges during each switching cycle. Within one cycle, the effective output signal can track the control reference. By varying the pulse width of the clock, the duty cycle of the pulse will change, influencing the THD value accordingly. For the rectangular pulse train with the duty cycle, μ (sometimes called the cyclic ratio), the THD_F formula [32] is as Eq. (5).

$$THD_F(\mu) = \sqrt{\frac{\mu(1-\mu)\pi^2}{2sin^2\pi\mu} - 1}, \qquad 0 < \mu < 1 \tag{5}$$

Theoretically, the THD value will reach its minimum when the signal becomes symmetrical μ=0.5. Figure 4 depicts the theoretical THD as a function of cyclic ratio (duty cycle) μ, and of filter's order, p computed accordingly to the analytical residue-based method in [32]. The THD decreases almost linearly with p in logarithmic scale; additionally, the closer the pulse train is to the square wave, the faster the THD decreases with order p [32].

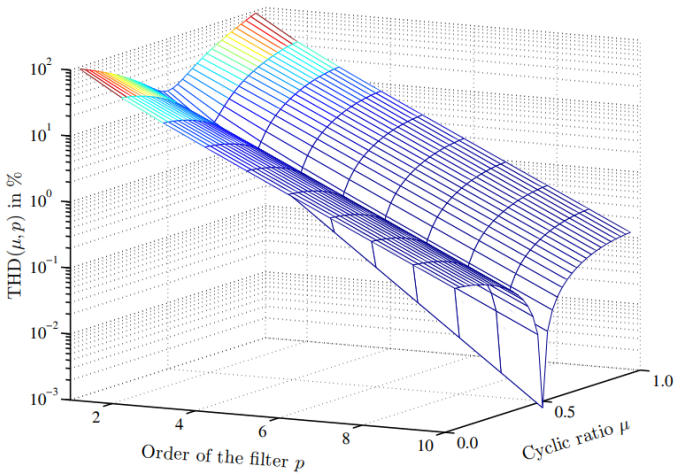

Fig. 4. Theoretical THD as a function of cyclic ratio (duty cycle) μ and of filter's order p computed accordingly to the analytical residue-based method [32]

Figure 5 depicts the control pulses generated by varying the widths of clock pulses. Meanwhile, Table 2 presents the relationship between the clock pulse width and the THD value of the supply currents compensated by the SAPF. From Table 2, when the clock pulse width is 16.7% and 33.3% of the clock period, the number of control pulses measured from 2s until 2.0005s is 6 and 7, respectively. This lower number of control pulses will significantly affect the THD value to be more than 5%, which is 5.94% and 5.61%, respectively. This condition is not favourable as it did not meet the requirement of IEEE Std-519-2014 [33], where the THD must be at least lower than 5%.

Table 2
THD values of supply currents when the SAPF using OCC with various clock pulse width

Clock Pulse Width (No of Samples)	No of Control Pulses (From 2s to 2.0005s)	THD%
1 (16.7%)	6	5.94%
2 (33.3%)	7	5.61%
3 (50%)	14	3.99%

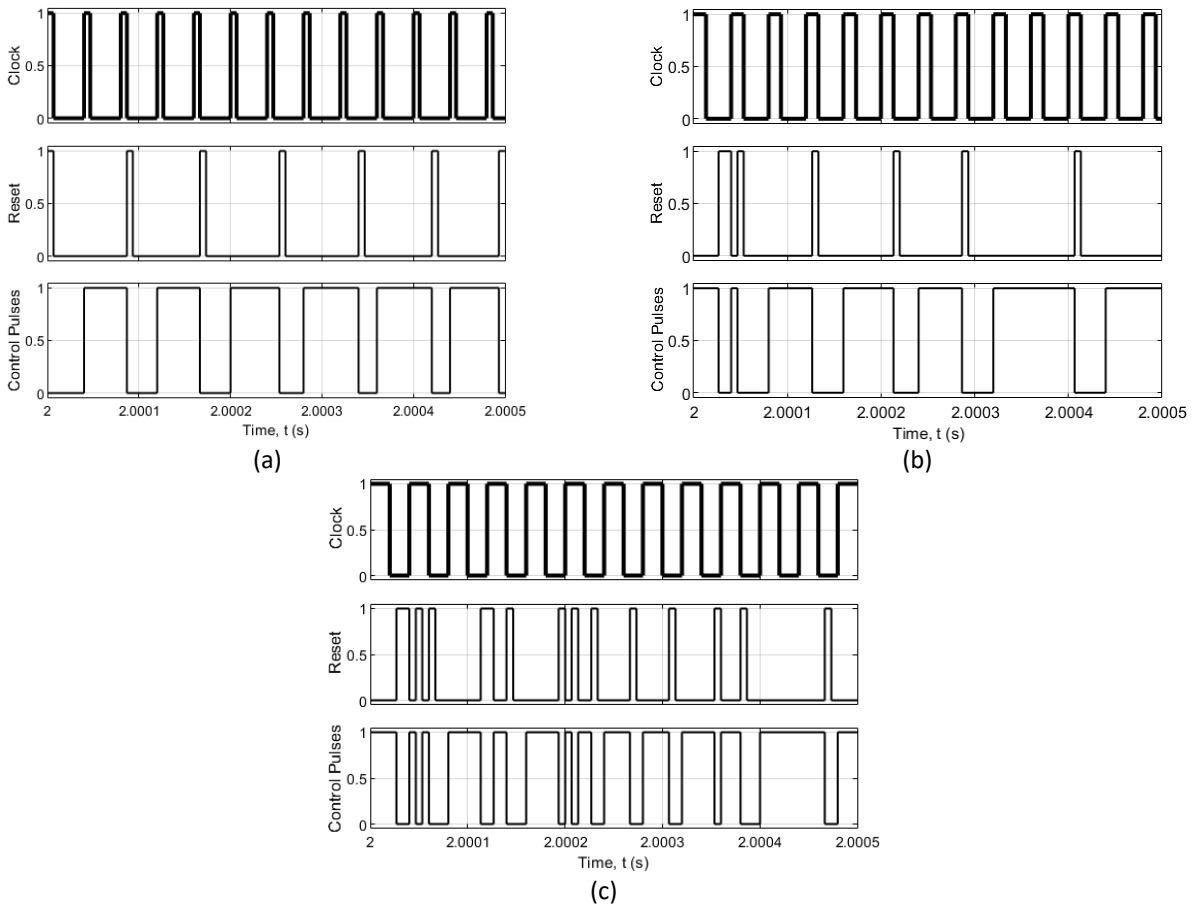

Fig. 5. Generated control pulses when the clock pulse width is (a)16.7%, (b)33.3% and (c)50% of the clock period

However, when the clock pulse width is set to 3, which is 50% of the clock period, the number of pulses increases drastically to 14. Eventually, it reduces the THD value to 3.99%, below than IEEE standard THD value of 5%. It provides the best THD value because the controller can reflect more

dynamic control pulses. In simple terms, when the clock width pulse is 50% of the clock period, it affects the controller's sensitivity, making it more sensitive and responsive to system changes. As a result, in the HOCPIC development, the 50% clock pulse width was chosen to maximise the controller operation and improve the SAPF performance.

4.2 The Harmonic Current Compensation using SAPF based HOCPIC Current Control Algorithms

Figure 6(a) depicts the simulation of voltage and current waveforms before SAPF is applied to the system. It illustrates that the source current is not sinusoidal due to numerous harmonic components. The THD value of the distorted supply current is 42.65%. Figure 6(b) shows the voltage and current waveforms after implementing the SAPF-based HOCPIC, while Figure 6(c) shows the voltage and current waveforms using the SAPF-based OCC. The source current is nearly sinusoidal for both conditions with a low current ripple. The SAPF's injection current has compensated for the harmonic current content. Therefore, it proved that the SAPF using HOCPIC and the SAPF using OCC could effectively compensate for the harmonic currents. Table 3 displays a compilation of THD values of supply current and the system's power factor before and after applying the SAPF using different current control algorithms.

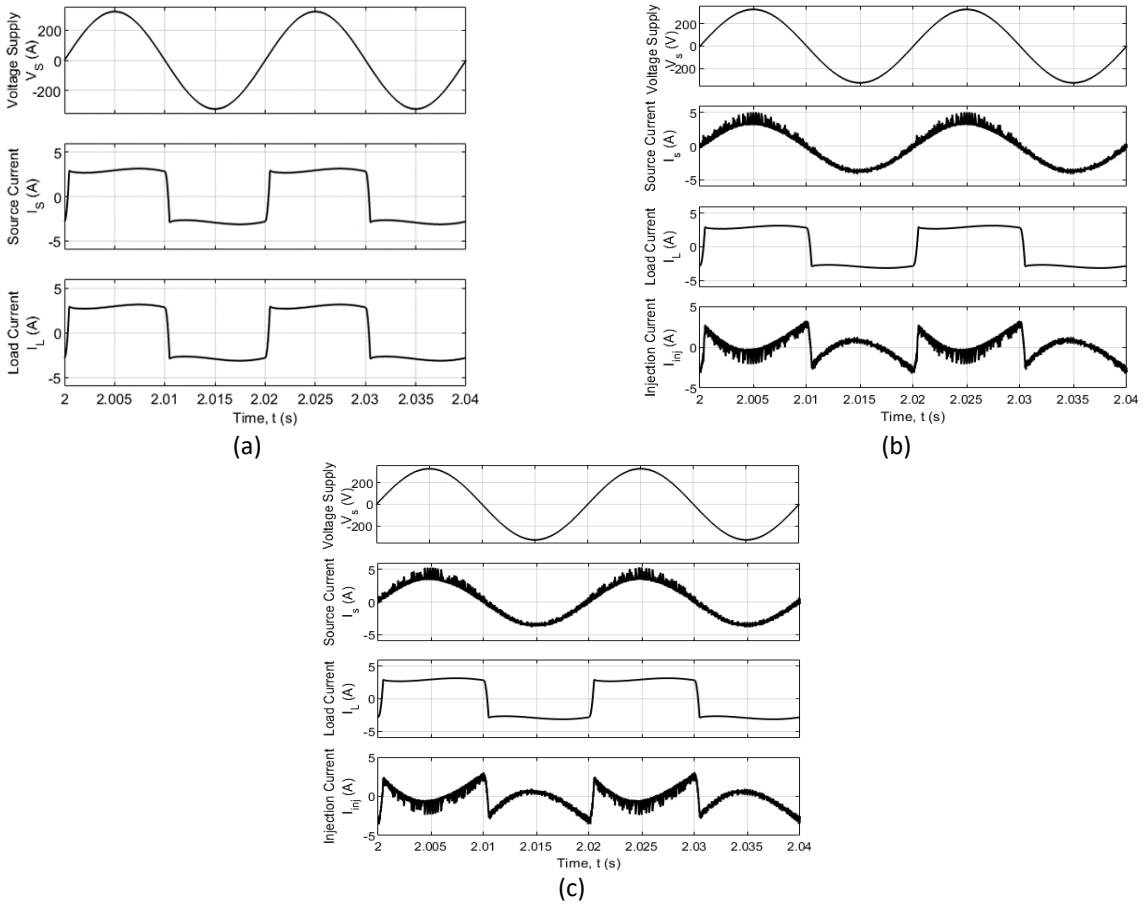

Fig. 6. Waveform result (a) before compensation, (b) after compensation using SAPF based HOCPIC and (c) after compensation using SAPF based OCC

Table 3
The compilation of results

Loop of Operation	Power Factor	THD%
Before using SAPF	0.9091	42.65%
After using SAPF-based HOCPIC	0.9885	3.20%
After using SAPF-based OCC	0.9864	3.99%

After applying the SAPF using HOCPIC, the power factor is improving from 0.9091 to 0.9885. Besides, the THD value of the supply current is reduced from 42.65% to 3.20% using the SAPF-based HOCPIC and 3.99% when using the SAPF-based OCC. According to the difference in the THD percentage, the result has verified that the SAPF-based HOCPIC performs better in compensating harmonic currents. Despite the results, both hybrid and conventional OCC can regulate the SAPF's injection current to reduce the THD value of the supply current below 5%. However, in terms of operational effectiveness in compensating harmonic currents, the SAPF-based HOCPIC outperforms OCC.

Figure 7 shows the harmonics spectrum of the supply current before and after implementing the SAPF-based HOCPIC and OCC. It can be observed that the individual odd harmonic percentage before compensation has an elevated harmonic spectrum and does not meet all the standard requirements. Meanwhile, the individual odd harmonics percentage after compensation using the SAPF-based HOCPIC and OCC meets the standard requirement of IEEE-519. The supply current compensated by the SAPF-based OCC has a higher individual harmonic percentage than being compensated by the SAPF-based HOCPIC. As for the SAPF-based OCC, the harmonic content of the third order is less than the fifth and seventh orders, which can happen in a single-phase proposed switching method. In addition, the authors in [34] also show that their robust switching rule design for single-phase SAPF can have a harmonic content of the third order less than the fifth and seventh orders.

Moreover, the supply current compensated by the SAPF-based HOCPIC has a higher individual harmonic percentage at the 17^{th} harmonic order. Thus, this shows that the SAPF-based HOCPIC can compensate for the lower order of harmonics components better than the SAPF-based OCC. As a result, it improves the THD value of the supply current further.

As previously stated, HOCPIC outperforms OCC due to OCC's incapability to tune the current error signal dynamically. Figure 8 shows the error current signal used by the HOCPIC and OCC to generate their control pulses. It is observed that there is a noticeable difference in the error current signal produced before and after inserting the PI controller. This PI controller in HOCPIC helps to tune the error signal by minimising the current error signal and eventually improves the SAPF operation in compensating harmonic components.

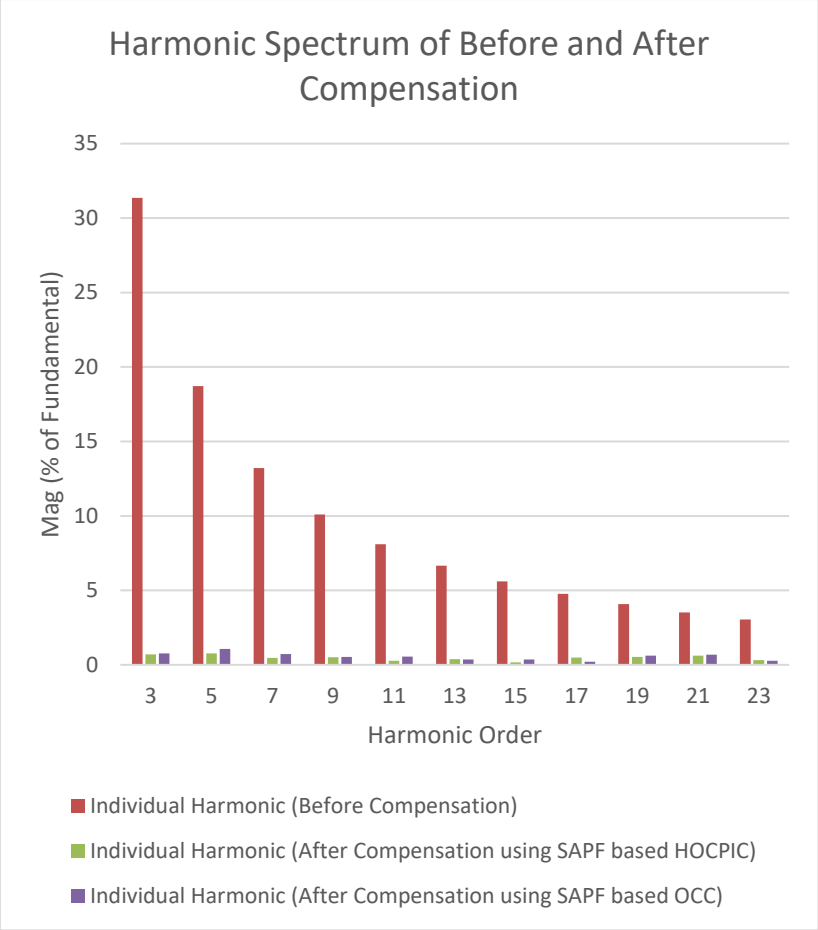

Fig. 7. Harmonic spectrum before and after harmonic compensation

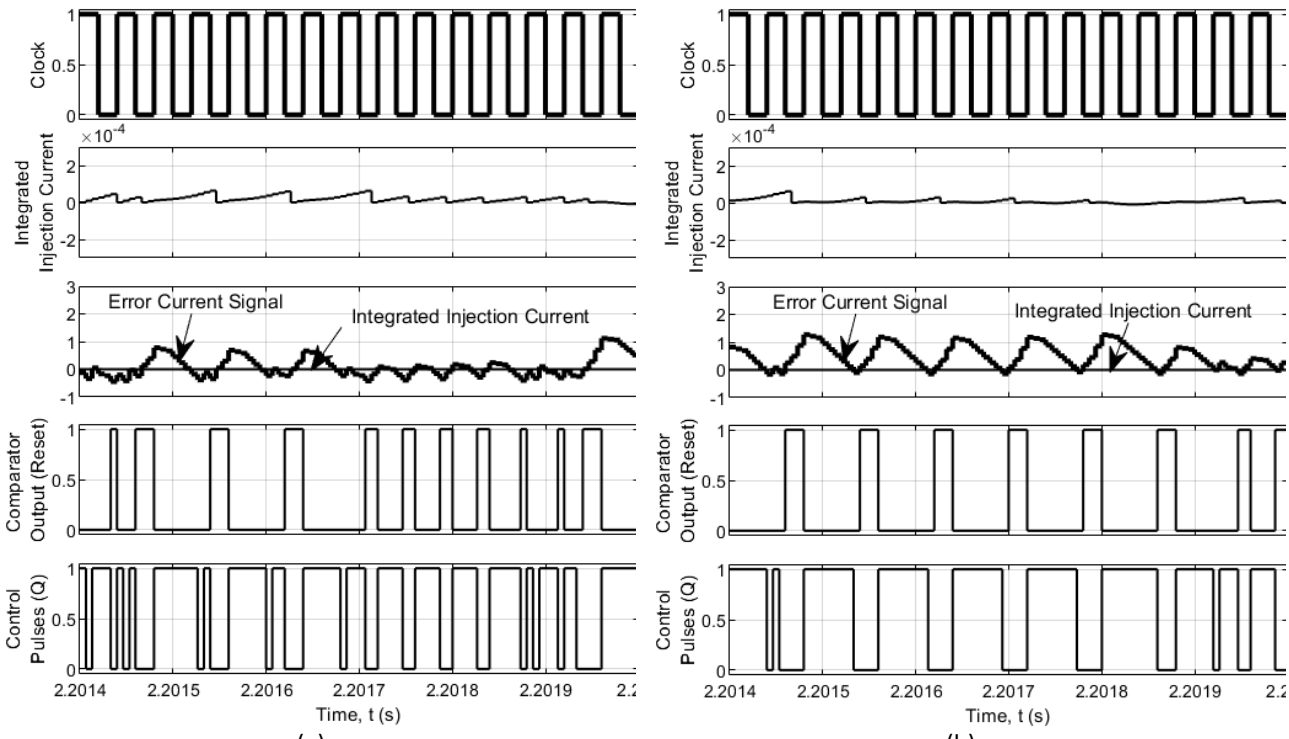

Fig. 8. Error current signal used by the (a)HOCPIC and (b)OCC to generate the control pulses

4.3 The THD of Supply Currents with Variable Nonlinear Load

The variable nonlinear load is constructed using variable resistive and fixed inductive elements. Table 4 displays the outcomes of the THD of the supply current using the variable nonlinear load. The present nonlinear inductive load comprises a resistor and inductor with a value of 70Ω and 0.8H, respectively. Upon reducing the resistor load to 60Ω, the THD of the supply current was observed to decrease from 3.20% to 3.12% for SAPF-based HOCPIC and from 3.99% to 3.46% for SAPF-based OCC. Nevertheless, upon increasing the resistor load to 80Ω, the THD of the supply current escalates to 3.39% for SAPF-based HOCPIC and 4.40% for SAPF-based OCC. In simple terms, the lower the resistor load, the lower the THD of the supply current. Furthermore, optimisation is required if a greater resistor load is utilised since the THD will might exceed the IEEE Std-519 limit of 5%.

Table 4
The THD of supply currents with varying resistor load

Nonlinear Load	THD% of SAPF-based HOCPIC	THD% of SAPF-based OCC
60 Ω and 0.8 H	3.12%	3.46%
70 Ω and 0.8 H	3.20%	3.99%
80 Ω and 0.8 H	3.39%	4.40%

5. Conclusions

The proposed SAPF-based HOCPIC reduces the THD of the supply current to 3.20% compared with 3.99% when using the SAPF-based OCC. Thus, it proves that SAPF-based HOCPIC had outperformed OCC in compensating harmonic currents due to the error minimisation approach. In addition, the SAPF-based HOCPIC has a simple control circuit that is easy to implement, making it a cost-effective and reliable solution for power quality control.

Acknowledgement
This research was not funded by any grant.

References
[1] Imam, Amir A., R. Sreerama Kumar, and Yusuf A. Al-Turki. "Modeling and simulation of a PI controlled shunt active power filter for power quality enhancement based on PQ theory." *Electronics* 9, no. 4 (2020): 637. https://doi.org/10.3390/electronics9040637
[2] Pinyol, Ramon. "Harmonics: Causes, effects and minimization." *Salicru white papers* (2015).
[3] Singh, Bhim, Kamal Al-Haddad, and Ambrish Chandra. "A review of active filters for power quality improvement." *IEEE transactions on industrial electronics* 46, no. 5 (1999): 960-971. https://doi.org/10.1109/41.793345
[4] Bingham, Richard P. "Harmonics-understanding the facts." *Dranetz Technologies* (1994).
[5] Motta, Lukas, and Nicolas Faundes. "Active/passive harmonic filters: Applications, challenges & trends." In *2016 17th International Conference on Harmonics and Quality of Power (ICHQP)*, pp. 657-662. IEEE, 2016. https://doi.org/10.1109/ICHQP.2016.7783319
[6] Chen, Yang, and Keyue Smedley. "Parallel Operation of One-Cycle Controlled Three-Phase Active Power Filter." In *Conference Record of the 2006 IEEE Industry Applications Conference Forty-First IAS Annual Meeting*, vol. 1, pp. 161-168. IEEE, 2006. https://doi.org/10.1109/IAS.2006.256500
[7] Mohd Zainuri, Muhammad Ammirrul Atiqi, Mohd Amran Mohd Radzi, Azura Che Soh, Norman Mariun, Nasrudin Abd Rahim, Jiashen Teh, and Ching-Ming Lai. "Photovoltaic integrated shunt active power filter with simpler ADALINE algorithm for current harmonic extraction." *Energies* 11, no. 5 (2018): 1152. https://doi.org/10.3390/en11051152

[8] Rahman, NFA Abdul, and SZ Mohammad Noor. "A new approach for single-phase shunt active power filter (SSAPF) operation." In *2012 International Conference on Power Engineering and Renewable Energy (ICPERE)*, pp. 1-6. IEEE, 2012. https://doi.org/10.1109/ICPERE.2012.6287234

[9] Ramu, Dasari, Chinta Narendra Kumar, Chunduri Rambabu, and Andhra Pradesh Tadepalligudem Tadepalligudem. "One Cycle Control Of Shunt Active Power Filter."

[10] Nagaprasad, Sattineni, Naveen Bolisetti, and P. Ram Prasad. "Modified One Cycle Controlled Scheme for Single-Phase Grid Connected Pv-Fc Hybrid System." https://doi.org/10.9790/1676-0865160

[11] Gautam, Samir, Pei Yunqing, Muhammad Kashif, Yubaraj Kafle, and Liu Yibo. "DC side voltage control consideration for single phase shunt active power filter for harmonic and reactive power compensation." *Journal of Electrical Engineering* 15, no. 4 (2015): 11-11. https://doi.org/10.11591/ijpeds.v4i1.4723

[12] Kazmierkowski, Marian P., and Luigi Malesani. "Current control techniques for three-phase voltage-source PWM converters: A survey." *IEEE Transactions on industrial electronics* 45, no. 5 (1998): 691-703. https://doi.org/10.1109/41.720325

[13] Smedley, Keyue M., and Slobodan Cuk. "One-cycle control of switching converters." *IEEE transactions on power electronics* 10, no. 6 (1995): 625-633. https://doi.org/10.1109/63.471281

[14] Bento, Aluízio AM, and Edison RC da Silva. "Application of One-Cycle Control technique for integrate power quality converter." In *2015 IEEE 13th Brazilian Power Electronics Conference and 1st Southern Power Electronics Conference (COBEP/SPEC)*, pp. 1-6. IEEE, 2015. https://doi.org/10.1109/COBEP.2015.7420046

[15] Huaiying, Cheng, Li Wenjuan, and Jiang Bo. "Simulation and experiment of single-phase APF with one-cycle control." In *Proceedings of 2013 2nd International Conference on Measurement, Information and Control*, vol. 2, pp. 1031-1034. IEEE, 2013. https://doi.org/10.1109/MIC.2013.6758135

[16] Bento, Aluisio AM, Luís FC Monteiro, and Edison RC da Silva. "Fast response one-cycle control strategy for three-phase shunt active power filter." In *2017 IEEE Southern Power Electronics Conference (SPEC)*, pp. 1-7. IEEE, 2017. https://doi.org/10.1109/SPEC.2017.8333654

[17] Ferreira, Armando José Gomes Abrantes. "Digital one-cycle control technique with grid voltage measurement applied to three-phase power factor corrected rectifiers and active power filters." (2019).

[18] Ramu, Dasari, Chinta Narendra Kumar, Chunduri Rambabu, and Andhra Pradesh Tadepalligudem Tadepalligudem. "One Cycle Control Of Shunt Active Power Filter."

[19] Sreeraj, E. S., E. K. Prejith, and Kishore Chatterjee. "One cycle controlled active harmonic filter." In *IECON 2012-38th Annual Conference on IEEE Industrial Electronics Society*, pp. 621-626. IEEE, 2012. https://doi.org/10.1109/IECON.2012.6388756

[20] Kianmanesh, Amir Masuod, and Ali Akhavan. "Power Control of Grid-Connected Inverters Using One-Cycle Control Method for PV Systems." In *2020 Zooming Innovation in Consumer Technologies Conference (ZINC)*, pp. 253-258. IEEE, 2020. https://doi.org/10.1109/ZINC50678.2020.9161434

[21] Salazar, Andres, Rodrigo Teixeira, Werbert da Silva, Guilherme Pillon, João Carvalho Neto, Elmer Villarreal, and Alberto Lock. "One Cycle Control of A PWM Rectifier a new approach." (2020). https://doi.org/10.3390/en13205523

[22] Sreeraj, E. S., E. K. Prejith, Kishore Chatterjee, and Santanu Bandyopadhyay. "An active harmonic filter based on one-cycle control." *IEEE Transactions on Industrial Electronics* 61, no. 8 (2013): 3799-3809. https://doi.org/10.1109/TIE.2013.2286558

[23] Saifizi, M., M. I. Fahmi, M. Othman, Wan Azani Mustafa, M. Z. Aihsan, M. R. Manan, and Azri A. Aziz. "Implementation of Two-Stage Multilevel Inverter System Using PIC Controller." *Journal of Advanced Research in Applied Sciences and Engineering Technology* 28, no. 2 (2022): 41-55. https://doi.org/10.37934/araset.28.2.4155

[24] Li, Lan, and Zeng-shang Kang. "Application of one-cycle control based on active power filter." In *Conference of the 2nd International Conference on Computer Science and Electronics Engineering (ICCSEE 2013)*, pp. 135-138. Atlantis Press, 2013. https://doi.org/10.2991/iccsee.2013.36

[25] Khalid, Saifullah, and Sudhanshu Verma. "THD and compensation time analysis of three-phase shunt active power filter using adaptive mosquito blood search algorithm (AMBS)." *International Journal of Energy Optimization and Engineering (IJEOE)* 8, no. 1 (2019): 25-46. https://doi.org/10.4018/IJEOE.2019010102

[26] Khalid, Saifullah. "Performance evaluation of Adaptive Tabu search and Genetic Algorithm optimized shunt active power filter using neural network control for aircraft power utility of 400 Hz." *Journal of Electrical Systems and Information Technology* 5, no. 3 (2018): 723-734. https://doi.org/10.1016/j.jesit.2017.04.003

[27] Khalid, Saifullah. "Optimized aircraft electric control system based on adaptive tabu search algorithm and fuzzy logic control." *Indonesian Journal of Electrical Engineering and Informatics (IJEEI)* 4, no. 3 (2016): 149-164. https://doi.org/10.11591/ijeei.v4i3.221

[28] Khalid, Saifullah. "THD and compensation time analysis of three-phase shunt active power filter using adaptive Spider Net Search Algorithm (ASNS)." *International Journal of Computing and Digital Systems* 5, no. 06 (2016). https://doi.org/10.12785/IJCDS/050607

[29] Khalid, Saifullah. "THD and Compensation Time Analysis of Three-Phase Shunt Active Power Filter Using Adaptive Spider Net Search Algorithm (ASNS) for Aircraft System." *Journal of Machine Intelligence* 2, no. 1 (2017): 1-6. https://doi.org/10.12785/IJCDS/050607

[30] Habbi, Hanan Mikhael D., Hussein Jalil Ajeel, and Inaam Ibrahim Ali. "Speed control of induction motor using PI and V/F scalar vector controllers." *International Journal of Computer Applications* 151, no. 7 (2016): 36-43. https://doi.org/10.5120/ijca2016911831

[31] Kaushal, Jitender, and Prasenjit Basak. "Power quality control based on voltage sag/swell, unbalancing, frequency, THD and power factor using artificial neural network in PV integrated AC microgrid." *Sustainable Energy, Grids and Networks* 23 (2020): 100365. https://doi.org/10.1016/j.segan.2020.100365

[32] Blagouchine, Iaroslav V., and Eric Moreau. "Analytic method for the computation of the total harmonic distortion by the Cauchy method of residues." *IEEE Transactions on communications* 59, no. 9 (2011): 2478-2491. https://doi.org/10.1109/TCOMM.2011.061511.100749

[33] Langella, Roberto, Alfredo Testa, and Et Alii. "IEEE recommended practice and requirements for harmonic control in electric power systems." In *IEEE Recommended Practice*. IEEE, 2014. https://doi.org/10.1109/IEEESTD.2014.6826459

[34] Lima, Vitor Leobet, and Tiago Jackson May Dezuo. "Robust Switching Rule Design for Single-Phase Shunt Active Power Filter." In *2021 Brazilian Power Electronics Conference (COBEP)*, pp. 1-4. IEEE, 2021. https://doi.org/10.1109/COBEP53665.2021.9684005